# Sphere motion in ordered three-dimensional foams

I. T. Davies[a)]

*Department of Computer Science, Aberystwyth University, Ceredigion SY23 3DB, United Kingdom and Institute of Mathematics and Physics, Aberystwyth University, Ceredigion SY23 3BZ, United Kingdom*

S. J. Cox

*Institute of Mathematics and Physics, Aberystwyth University, Ceredigion SY23 3BZ, United Kingdom*

(Received 9 September 2011; final revision received 25 January 2012; published 20 March 2012)

**Synopsis**

The effect of the interplay between surface tension and gravity on the sedimentation of objects in structured fluids is investigated by simulating the quasi-static motion of a spherical particle through an ordered foam. We describe the path which a sphere takes as it descends through bamboo (1,1,0), staircase (2,1,1), chiral (3,2,1), and double staircase (4,2,2) foams, and measure the degree of control of the sphere's motion that each foam offers. For an ordered foam contained within a vertical cylinder, the resulting sphere motion depends strongly on the structure itself, on how the films are deformed near the sphere, and on how the motion of the sphere deforms them further. For staircase and chiral foams, the distance that a sphere is pulled away from the center-line of the cylinder by the foam is found to depend on the Bond number with a power-law relation. By tilting the cylinder at an angle to the vertical, we show that there exists a critical tilt angle above which the sphere falls out of the foam. This angle is dependent on the choice of foam structure and the Bond number. For a sphere of given size and given Bond number in the ordered foams studied here, the greatest tilt can be imposed on the double staircase foam. © *2012 The Society of Rheology*.
[http://dx.doi.org/10.1122/1.3687415]

## I. INTRODUCTION

An area of application in which foams [Cantat *et al.* (2010); Weaire and Hutzler (1999)] find wide use is separation, using the process known as froth fractionation or flotation. When applied to the recovery of ores, the efficiency of the separation process is directly related to the profit that can be obtained, so that being able to predict the motion of particles in foams is of paramount importance [Neethling and Cilliers (2002)].

Another, more recent, use of foams is in microfluidics for sample testing [Whitesides and Stroock (2001)]. Small samples of gas (or liquid, in an emulsion, with properties very similar to that of a foam) can be pushed through narrow channels and re-directed at will. When the liquid content is low, the foams form ordered structures that have

[a)]Author to whom correspondence should be addressed; electronic mail: itd@aber.ac.uk

remarkable properties [Drenckhan *et al.* (2005); Raven and Marmottant (2009)], including the ability to switch between them by a single dislocation [Boltenhagen and Pittet (1998); Pittet *et al.* (1996)], which can be controlled, for example, purely by liquid fraction.

Here, we study the motion of a spherical particle in an ordered foam structure, with the aim of describing its motion and showing how it can be controlled by the choice of foam structure. For example, an appropriate choice of structure can keep the sphere in the center of the channel, even when gravity acts to pull it towards the side walls, or can cause the sphere to move in an oscillatory manner.

The flow of a foam past a sphere, and in particular its 2D equivalent, has been used as a testing ground for the validation of discrete simulations [Cox *et al.* (2006); Raufaste *et al.* (2007); Wyn *et al.* (2008)] and continuum models of foam [Cheddadi *et al.* (2011)] against experiments [Dollet *et al.* (2005a, 2005b); Lambert *et al.* (2005)]. In simulations, the different components of the force on an object embedded in the foam can be separated: the network of soap films pull on the object with a surface tension force; bubbles apply a pressure force to the object; and there is a viscous resistance to motion of the soap films over the object. The rich collection of elastic, plastic, and viscous responses of the foam, depending on flow-rate, mean that the network and pressure forces are asymmetric and have a nonzero resultant. For example, films stretch behind the object (elasticity), exerting a drag force on it, until the short films that connect them shrink in area to trigger a neighbor-switching T1 topological change (plasticity). Here, we use these mechanisms in elasto-plastic (quasi-static) simulations with the Surface Evolver [Brakke (1992)] to show how the drag and lift due to network and pressure forces can be used to control the descent of a sphere through a foam.

In the two-dimensional case, Raufaste *et al.* (2007) showed how the network drag force depends on the bubble area $A_b$, disc diameter $d_0$, line tension $\gamma_{2D}$, and effective liquid fraction $\Phi_l$,

$$F^n \sim \frac{\gamma_{2D} d_0}{\sqrt{A_b}\Phi_l^{1/4}}. \tag{1}$$

Thus sphere and bubble size are expected to have a large effect on the network force in the 3D case described here. The dependence of the pressure drag on these parameters is less clear: since bubble pressure increases with decreasing bubble size and the area over which the force acts increases with sphere diameter squared, we can expect that the pressure force will be low for large bubbles and small spheres.

The ordered foams that we use can be made by generating bubbles in a vertical cylinder [Boltenhagen and Pittet (1998); Pittet *et al.* (1996)]. The structure that results depends strongly on the ratio of cylinder radius to bubble size (defined as the radius of a sphere of the same volume), which we denote by $\lambda$. They can be described with a phyllotactic notation [Weaire and Hutzler (1999)], of which the first few, with which we shall be concerned here, are shown in Fig. 1: bamboo (1,1,0), consisting of parallel circular films; the staircase structure (2,1,1), with two bubbles in the unit cell, each filling half the cylinder; a chiral structure (3,2,1) with three bubbles in the unit cell; a double staircase structure (4,2,2) with four bubbles in the unit cell, and so on.

Consider first the bamboo structure, and in particular the motion of a sphere under gravity through an initially horizontal film confining a bubble of fixed volume (Fig. 2). Once the sphere meets the film [Fig. 2(b)], the pressure in the bubble below the film drops below that in the bubble above it, so that there is a net downward pressure force; in addition, the soap film pulls downwards on the sphere. Thus network and pressure forces both

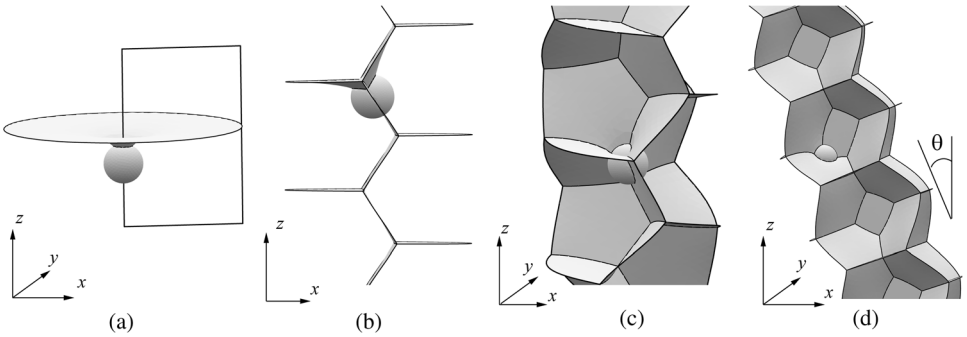


**FIG. 1.** Snapshots of a sphere in four ordered cylindrical foams: (a) A bamboo (1,0,0) foam, through which the sphere moves vertically downwards ($z$ direction). The rectangular region shows the view in the axisymmetric calculation of Fig. 2(f). (b) A staircase (2,1,1) foam, where the sphere's motion is in the $x$ and $z$ directions only (the $y$-axis is into the page). (c) A chiral (3,2,1) foam in which the sphere spirals in a three-dimensional motion. (d) A double staircase (4,2,2) foam with the cylinder tilted in the ($x$, $z$) plane so that its center-line makes an angle $\theta$ with the $z$-axis.

act to increase the velocity of the sphere. This is, however, a small effect, because the film moves to a position close to the equator of the sphere, so as to satisfy the 90° condition. When the film touches the equator it becomes horizontal again [Fig. 2(c)], although it is slightly higher than at the start because the volume in the bubble is conserved, and both forces are zero. Once the center of the sphere moves below the film, the pressure and network forces retard the sphere motion [Figs. 2(d) and 2(e)]. The asymmetry of the motion then becomes apparent because the film now moves right up to the north pole before detachment [Fig. 2(f)].

Clearly, if the weight of the sphere is too small, this asymmetry can cause it to be held by the foam. The trapping of spheres by a bamboo foam was examined by Le Goff *et al.* (2008); note that in the noninertial case considered here, the deformation of the films is much smaller. In what follows, we ensure that the sphere weight is sufficiently large that this does not happen. In effect, this means that the Bond number (defined below) of the flow is always greater than one. Figure 2(g) shows that the network force is an order of magnitude greater than the pressure contribution to the force in this case.

We first describe the 3D simulations (Sec. II) which allow us to predict sphere motion in ordered foams. We show how the deviation of the sphere of given radius and density from the center-line of a vertical cylinder is described purely by the Bond number (Sec. III). We then investigate the degree by which a cylinder containing an ordered structure can be tilted without the sphere leaving the center of the cylinder (Sec. IV).

## II. SIMULATION METHODOLOGY

The Surface Evolver allows us to resolve bubble pressures and film shapes and thus to measure both the network and pressure forces on the sphere independently. Dry ordered foam structures were constructed in a cylinder of radius 1.5, with axis in the $z$ direction. For nonchiral structures we employ periodic boundary conditions at the ends of the cylinder, while for the chiral (3,2,1) (for which we want to allow the structure to choose the degree of twist, which may *a priori* depend on the position of the sphere) we use free boundary conditions. Each ordered foam results from a different choice of the bubble volume $V$, which fixes the value of $\lambda$: it is equal to $\lambda = 1.33$ ($V = 6.06$) for the (2,1,1) foam, 1.42 ($V = 4.95$) for the (3,2,1) foam, and 1.58 ($V = 3.53$) for the (4,2,2) foam.

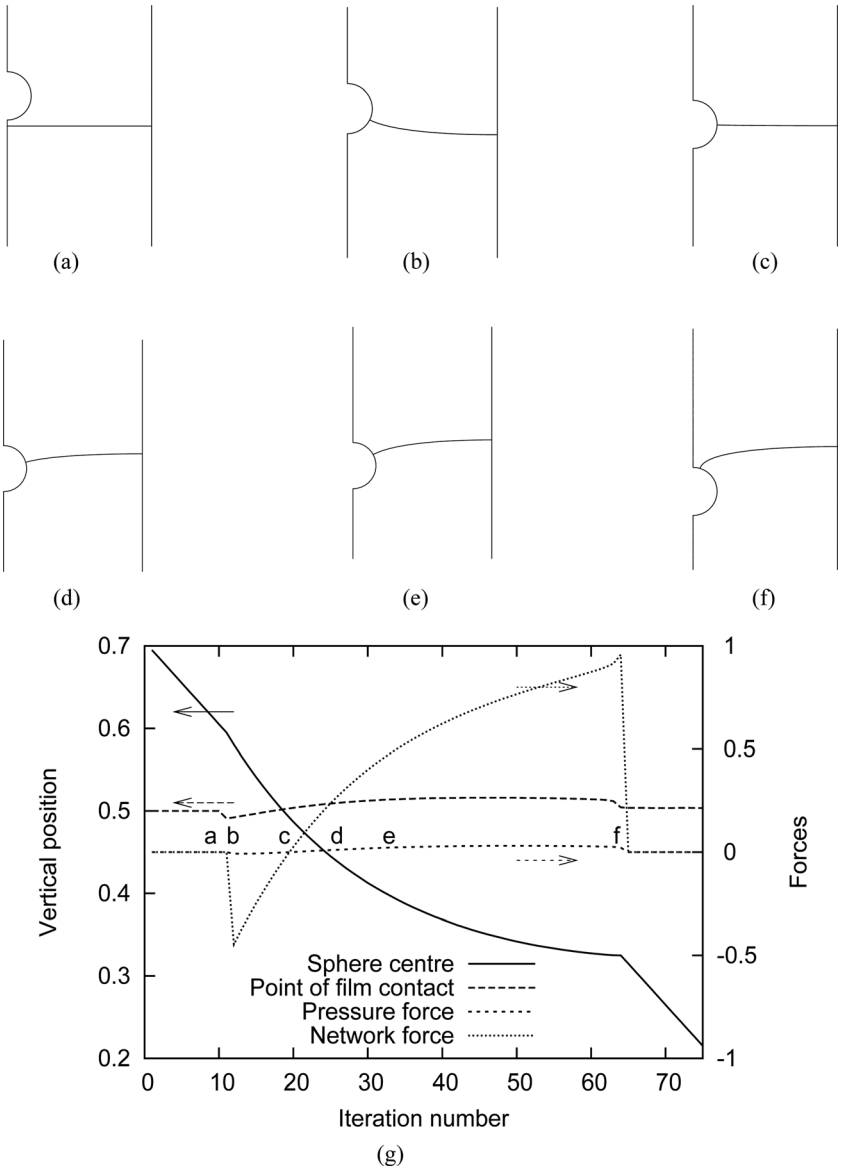


**FIG. 2.** Axisymmetric simulation of a sphere moving downwards under gravity through one film of a bamboo foam; the images represent a slice through the structure shown in Fig. 1(a). The sphere has unit weight, the ratio of sphere radius to cylinder radius is 1 to 6, and the film has unit tension. Images are shown at iteration (a) 8 (sphere above film), (b) 11 (lowest point of contact between film and sphere), (c) 18 (film meets equator), (d) 25, (e) 32, and (f) 63 (highest point of contact). (g) As a function of iteration number we show the vertical position of the center of the sphere, the vertical position of the point of contact between the film and the sphere, and the pressure and network contributions to the drag force on the sphere. The letters correspond to the images above.

The initial structure is tessellated with triangular facets. We use up to $10^4$ triangles, which gives a sufficiently accurate representation of the foam structure to resolve film curvature and pressures, without making the computational burden too great. The surface area is then minimized subject to the volume constraint imposed on each bubble.

Topological changes are triggered when a film shrinks below a critical cut-off area $A_c = 2 \times 10^{-3}$; this defines an effective liquid fraction [Raufaste *et al.* (2007)], here appropriate for a dry foam, $\Phi_l < 10^{-3}$.

The network and pressure forces on the sphere are calculated as described by Wyn *et al.* (2008), but extended to 3D in the natural way. The network force ($\vec{F}^n$) exerted on the sphere is the sum over all film edges $i$ contacting it; each pulls with a force equal to twice the value of surface tension, $2\gamma$, since the films represent a gas-liquid-gas interface, over the length $l_i$ of the edge. This force is applied in the direction of the outward normal to the sphere at the midpoint of the edge, denoted $\vec{n}_i$. Thus, the resultant network force is given by,

$$\vec{F}^n = 2\gamma \sum_i l_i \vec{n}_i. \tag{2}$$

The pressure force ($\vec{F}^p$) is calculated by summing over all facets $k$ of the sphere the pressures $p_k$ in the bubbles that contact the sphere multiplied by each (planar) facet's area $A_k$ and outward normal $\vec{n}_k$,

$$\vec{F}^p = -\sum_k p_k A_k \vec{n}_k. \tag{3}$$

The minus sign results because the pressure force acts towards the center of the sphere.

The resultant force is, therefore,

$$\vec{F} = -\frac{4}{3}\pi \rho_s r_s^3 g \vec{z} + \vec{F}^p + \vec{F}^n, \tag{4}$$

where $\rho_s$ and $r_s$ denote the density and radius of the sphere, $g$ is the acceleration due to gravity, and $\vec{z}$ is a unit vector in the positive $z$ direction.

The motion of the sphere through each foam is quantified in terms of a dimensionless Bond number, $Bo$, relating the balance of surface tension effects to gravitational effects,

$$Bo = \frac{\rho_s g r_s^2}{\gamma}. \tag{5}$$

We work within the quasi-static regime, in which the motion of the sphere in the foam is assumed to be slow and steady. This allows for simplification of the governing equation for the motion of the sphere [Wyn *et al.* (2008)]. Briefly, we choose a small constant $\epsilon$, here taken equal to $1/(40Bo)$, which sets the effective time-scale for our simulations. At each iteration, the sphere is moved a small distance $\epsilon|\vec{F}|$ in the direction of the resultant force and the foam structure returned to equilibrium with the sphere fixed. The latter requires a total of 600 conjugate gradient steps, interspersed with tests for topological changes and upkeep of the tesselation.

## III. RESULTS: ORDERED FOAMS IN VERTICAL CYLINDERS

### A. Staircase foam (2,1,1)

Releasing a sphere into a staircase foam results in two-dimensional motion, dictated by the symmetry of the three-dimensional foam structure [Fig. 1(b)]. For small $Bo$, the periodicity of the structure causes the forces, and thus the sphere motion, to be oscillatory

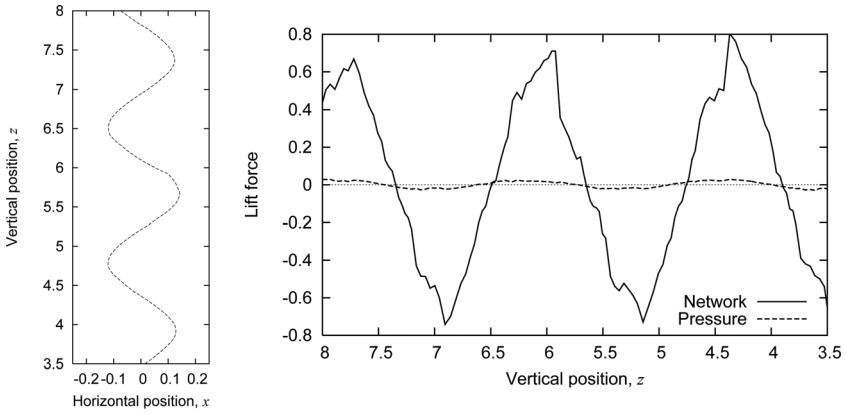


**FIG. 3.** Motion of a sphere in a staircase foam, in the case $Bo = 2.34$. (a) The position of the sphere oscillates in the $(x, z)$ plane, here with amplitude $a = 0.14$. (b) The network and pressure components of the (horizontal) lift force exerted on the sphere *versus* its vertical position.

[Fig. 3(a)]. The sphere is pulled to the right by films in contact with the right hand side of the cylinder and *vice-versa*. The films are deformed by the presence and passage of the sphere, which causes the bubble pressures to change. There is, therefore, a resultant pressure force, which acts in the same sense as the network force, but is much smaller in magnitude [Fig. 3(b)].

The staircase foam pulls the sphere from the center-line of the cylinder; how far the sphere is pulled away from the center-line is dependent on the interplay between surface tension and gravity, for example a lighter sphere will deviate a greater distance than a heavier sphere of the same radius. By varying the Bond number, we can quantify the amplitude of the motion (Fig. 4): the relation between the amplitude ($a$) and the Bond number can be fitted to the following power-law:

$$a = 0.29\, Bo^{-0.88}. \tag{6}$$

For small $Bo$, the surface tension of the films has a greater effect than the weight of the sphere, resulting in the sphere's path deviating by a fairly large amount from the center of the cylinder. For large $Bo$, gravity dominates, reducing the amplitude. The result is

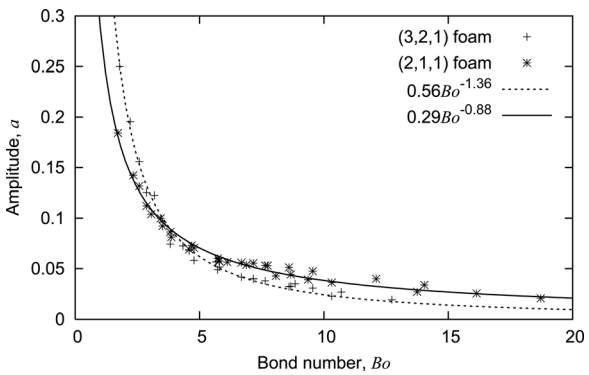


**FIG. 4.** The amplitude of the oscillatory motion of the sphere in the staircase and chiral foams *versus* Bond number. Also shown are power-law fits for each case.

independent of how the Bond number is varied, i.e., whether sphere radius or density is changed.

### B. Chiral foam (3,2,1)

Releasing a sphere from a central position at the top of a chiral (3,2,1) foam [Fig. 1(c)] results in a spiraling downward motion [Fig. 5(a)]. As for the staircase, the pressure contribution to the lift is much smaller than from the network. In the case shown, with $Bo = 2.58$, the sphere follows the column of Plateau borders close to the center-line of the cylinder. By viewing the path of the sphere from above [Fig. 5(a)], one can see that it resembles a triangular spiral. The angular shifts in this path are a signature of the chirality of the structure.

As for the staircase foam, the deviation of a sphere's path from the cylinder's center-line depends on the Bond number. The spiraling motion of a heavy sphere deviates less than that of a lighter sphere of the same size. Figure 4 shows that the maximum displacement of the sphere from the center of the cylinder can be fitted to a power-law in $Bo$:

$$a = 0.56\, Bo^{-1.36}. \tag{7}$$

If the Bond number is small, a sphere is pulled slightly further from the center-line than in the staircase foam. Conversely, at large Bond number a sphere remains closer to the center-line.

Having seen what happens when a sphere is released from a central position in the chiral foam, we consider what happens when the initial position of the sphere is varied, in order to quantify how far a sphere can be positioned from the center of the cylinder and still find a spiral path within the foam. This will allow us to make predictions concerning the range over which the foam can be used to control the motion of the sphere. In this case, we consider the descent of a light, small sphere ($Bo = 2.58$) from three noncentral positions, with the $(x, y)$ coordinates of the sphere's center at (0.2,0.2), (0.4,0.4), or (0.6,0.6). It can be seen in Fig. 5(b) that the first two positions are close enough to the center of the cylinder that the sphere finds the same path that it traveled when positioned

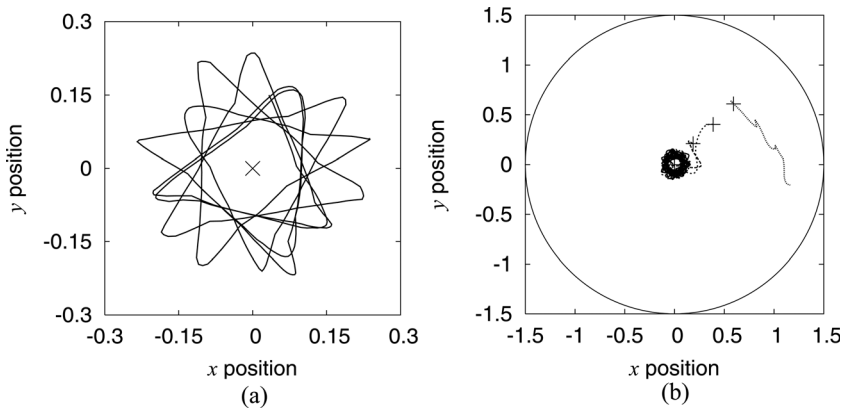


**FIG. 5.** Sphere motion in a chiral foam, with $Bo = 2.58$. (a) The path of a sphere which is initially positioned at the center of the top of the cylinder, viewed from above. (b) Tracking the path of the same sphere from three different, noncentral, initial positions. Each initial position is labeled with a cross. If the sphere starts too far away from the center then it moves towards the wall; otherwise it is brought back to the central region of the foam.

centrally in the cylinder. Therefore the same path will be found if the initial distance separating the centers of the sphere and the cylinder is less than about one-third of the cylinder's radius. If the sphere is initially further from the cylinder's center, then it moves towards the wall. In this case, any control that could be exerted over the motion of the particle is lost. The motion of the sphere towards the wall is the result of the films being deformed by the sphere and tilting towards the wall. Several other initial positions for the sphere were also tested and it was found that the resulting path of the sphere depends only on the radial coordinate of the initial position and not the angular coordinate.

### C. Double staircase foam (4,2,2)

A sphere dropped from the center of a double staircase (4,2,2) foam falls in a straight line (not shown). The motion of the sphere is directed by vertically aligned films positioned close to the center of the cylinder [see Fig. 1(d)], which prevent the sphere from moving towards the wall. The initial position of the sphere was varied away from the center of the cylinder and if the sphere starts "inside" the vertically aligned films then it returns to its vertical path. Otherwise it moves to the wall as above.

## IV. RESULTS: ORDERED FOAMS IN TILTED CYLINDERS

Here we investigate how far a cylinder containing an ordered foam can be tilted without a sphere falling to the wall. This is, in a sense, a measure of the stability conferred on the sphere's motion by the choice of foam structure. We anticipate a critical tilt angle $\theta_c$, dependent on the Bond number, above which the sphere falls out of the foam to rest on, or slide down, the wall. We measured this critical angle using the following trial-and-error method. A simulation was run with the cylinder tilted at a given angle $\theta$. Then, depending on whether or not the sphere remained within the foam and its distance from the wall reached a plateau, a new simulation was run with an increased $(\theta + 1^\circ)$ or decreased tilt angle $(\theta - 1^\circ)$. The critical value recorded for the tilt angle $(\theta_c)$ is the average of the smallest angle at which the sphere falls out of the foam and the greatest angle at which the foam supports the sphere.

### A. Staircase foam (2,1,1)

We tilt a cylinder containing a staircase foam in the same direction ($x$) as the oscillatory motion occurs, since there is little resistance to sphere motion in the $y$ direction, and investigate the relationship between the critical tilt angle and the Bond number. It can be seen in Fig. 6 that $\theta_c$ decreases with increasing $Bo$, which we fit with a power-law,

$$\theta_c = 17.28\, Bo^{-0.59}.$$

In this case, the cylinder can be tilted up to angles of between 5 and 12° while control over the motion of a sphere is retained.

### B. Chiral foam (3,2,1)

Repeating the procedure described above, we show that the degree of control we have over the spiraling motion of the sphere in the chiral foam is similar to that obtained in the staircase foam. The relationship between the critical angle and the Bond number is approximated by

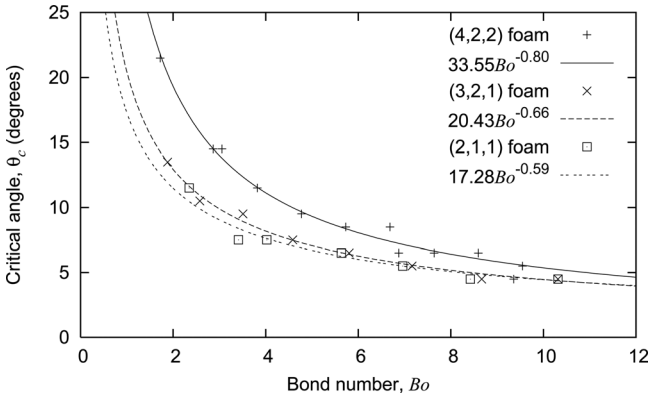


**FIG. 6.** We find the critical angle $\theta_c$ which is the maximum value for $\theta$ [see Fig. 1(d)] before the sphere falls out of the foam to touch the cylinder wall. The critical tilt angle for the staircase, chiral and double staircase foams decreases with increasing Bond number. The given fits to a power-law have an exponent that increases with $\lambda$.

$$\theta_c = 20.43\, Bo^{-0.66},$$

shown in Fig. 6. Here, the cylinder can be tilted up to angles of between 5 and 14° while maintaining control over the motion of a sphere.

### C. Double staircase foam (4,2,2)

Recall that the motion of a sphere through the double staircase (4,2,2) foam in a vertical cylinder was straight down. By tilting this foam, we show that it is possible to control the motion of the sphere for larger tilt angles than in the staircase and chiral foams, with the following fit to the dependence of critical angle on Bond number,

$$\theta_c = 33.55\, Bo^{-0.80},$$

shown in Fig. 6. For small Bond number ($Bo = 1.72$), it is possible to tilt the cylinder at an angle of 21° without losing control over the sphere motion. The greater degree of control here is due to the foam having more films in contact with the sphere compared to the other foams. The vertically aligned films along the center of this structure provide a slightly stronger support for the sphere as it descends through the cylinder. To increase the critical angle further, we would need to consider higher-order foams with smaller bubbles (larger $\lambda$), as in the experiments of Tobin *et al.* (2011).

## V. CONCLUSIONS

Investigating the motion of spherical particles through ordered foam structures provides an insight into the interplay between surface tension effects and gravity during sedimentation. Here we have shown how a sphere descends through bamboo (1,1,0), staircase (2,1,1), chiral (3,2,1), and double staircase (4,2,2) foams and measured the degree of control of the sphere's motion that each foam offers. For an ordered foam contained within a vertical cylinder, the resulting sphere motion depends strongly on the structure itself, on

how the films are deformed near the sphere, and on how the motion of the sphere deforms them further.

For a staircase foam, the motion is two-dimensional. A spiraling descent is observed in a chiral foam and in the double staircase foam a sphere falls straight down, as in a bamboo foam. For staircase and chiral foams, the distance that a sphere is pulled away from the center-line of the cylinder by the foam is found to depend on the Bond number through a power-law relation.

By tilting the cylinder at an angle to the vertical, we show that there exists a critical angle above which the sphere falls out of the foam. This angle is dependent on the choice of foam structure and the Bond number. For a sphere of given size and given Bond number in the ordered foams studied here, the greatest tilt can be imposed on the double staircase foam, since the bubbles are smaller and so more films are in contact with the sphere at all times.

We expect that our conclusions could be confirmed by experiment. These ordered foams have low values of $\lambda$, meaning that it should be possible to track the position of a falling spherical bead without recourse to tomography, although it may be necessary to use mirrors or a pair of cameras to observe full details of the motion. An ordered foam can be obtained by carefully calibrating the flow of gas into a reservoir of surfactant solution beneath a glass cylinder so that the values for $\lambda$ are matched. With a cylinder of radius around 15 mm, the required bubble sizes will be of the order of $10^3$ mm$^3$, and a sphere of radius 3 mm, and density 950 kg/m$^3$ (taking $Bo \approx 1.7$) would be appropriate.

We expect that changes in the liquid fraction of the foam will affect the drag and lift forces, and thus the sphere motion, only weakly. Raufaste *et al*. (2007) showed in 2D that increasing the liquid fraction reduces the forces exerted on a solid object since T1 events are more easily triggered on its boundary. However, for the ordered foams we consider here, T1 events do not occur, and the motion of a sphere is governed by the orientation of the soap films and the bubbles' shape. Increasing the liquid fraction slightly will only impose slight changes on the shape of bubbles and orientation of the films, so that its effect on sphere motion will also be minimal.

Including the effect of viscosity may be more significant, since this affects the angles at which films meet the sphere and therefore the network force. It could also lead to rotation of the sphere as it descends through the ordered structures.

At low $\lambda$, we expect the order of magnitude of the forces on a sphere in a *disordered* foam to be close to the values given here (note that disorder does not, for example, explicitly enter Eq. (1)). By making the bubbles smaller (increasing the value of $\lambda$), it would be increasingly difficult to generate an ordered foam, but the techniques described here will remain appropriate for an investigation of the motion of a sphere in a disordered foam.

Finally, we note that the structures described here can be made in cylinders of different cross-section [Tobin *et al*. (2011)], which may provide further applications of this work.

## ACKNOWLEDGMENTS

The authors thank K. Brakke for developing, distributing and supporting the Surface Evolver, and F. Graner for stimulating discussions. Financial support is gratefully acknowledged from EPSRC (EP/D071127/1) and the Research Institute for Visual Computing (RIVIC).

## References


Boltenhagen, P., and N. Pittet, "Structural transitions in crystalline foams," Europhys. Lett. **41**, 571–576 (1998).

Brakke, K., "The Surface Evolver," Exp. Math. **1**, 141–165 (1992).

Cantat, I., S. Cohen-Addad, F. Elias, F. Graner, R. Höhler, O. Pitois, F. Rouyer, and A. Saint-Jalmes, *Les mousses-structure et dynamique* (Belin, Paris, 2010).

Cheddadi, I., P. Saramito, B. Dollet, C. Raufaste, and F. Graner, "Understanding and predicting viscous, elastic, plastic flows," Euro. Phys. J. E **34**, 1 (2011).

Cox, S. J., B. Dollet, and F. Graner, "Foam flow around an obstacle: simulations of obstacle-wall interaction," Rheol. Acta **45**, 403–410 (2006).

Dollet, B., F. Elias, C. Quilliet, A. Huillier, M. Aubouy, and F. Graner, "Two-dimensional flows of foam: Drag exerted on circular obstacles and dissipation," Colloids Surf., A **263**, 101–110 (2005a).

Dollet, B., F. Elias, C. Quilliet, C. Raufaste, M. Aubouy, and F. Graner, "Two-dimensional flow of foam around an obstacle: Force measurements," Phys. Rev. E **71**, 031403 (2005b).

Drenckhan, W., S. J. Cox, G. Delaney, H. Holste, and D. Weaire, "Rheology of ordered foams—On the way to discrete microfluidics," Colloids Surf. A **263**, 52–64 (2005).

Lambert, J., I. Cantat, R. Delannay, A. Renault, F. Graner, J.A. Glazier, I. Veretennikov, and P. Cloetens, "Extraction of relevant physical parameters from 3D images of foams obtained by X-ray tomography," Colloids Surf. A **263**, 295–302 (2005).

Le Goff, A., L. Courbin, H. A. Stone, and D. Quéré, "Energy absorption in a bamboo foam," Europhys. Lett. **84**, 36001 (2008).

Neethling, S. J., and J. J. Cilliers, "Solids motion in flowing froths," Chem. Eng. Sci. **57**, 607–615 (2002).

Pittet, N., P. Boltenhagen, N. Rivier, and D. Weaire, "Structural transitions in ordered, cylindrical foams," Europhys. Lett. **35**, 547–552 (1996).

Raufaste, C., B. Dollet, S. Cox, Y. Jiang, and F. Graner, "Yield drag in a two-dimensional foam flow around a circular obstacle: Effect of liquid fraction," Eur. Phys. J. E **23**, 217–228 (2007).

Raven, J.-P., and P. Marmottant, "Microfluidic crystals: Dynamic interplay between rearrangement waves and flow," Phys. Rev. Lett. **102**, 084501 (2009).

Tobin, S., J. Barry, A. Meagher, B. Bulfin, C. O'Rathaille, and S. Hutzler, "Ordered polyhedral foams in tubes with circular, triangular and square cross-section," Colloids Surf. A **382**, 24–31 (2011).

Weaire, D., and S. Hutzler, *The Physics of Foams* (Clarendon, Oxford, 1999).

Whitesides, G. M., and A. D. Stroock, "Flexible methods for microfluidics," Phys. Today **54**, 42–48 (2001).

Wyn, A., I. T. Davies, and S. J. Cox, "Simulations of two-dimensional foam rheology: Localization in linear couette flow and the interaction of settling discs," Eur. Phys. J. E **26**, 81–89 (2008).